Electronic and magnetic properties of $Ga_{1-x}Mn_xAs$: Role of Mn defect bands

Yu-Jun Zhao, W. T. Geng, K. T. Park,* and A. J. Freeman
Department of Physics and Astronomy, Northwestern University, Evanston Illinois 60208
(Received 27 November 2000; revised manuscript received 29 January 2001; published 25 June 2001)

$Ga_{1-x}Mn_xAs$ and related semiconductors are under intense investigation for the purpose of understanding the ferromagnetism in these materials, pursuing higher T_C, and, finally, for realizing semiconductor electronic devices that use both charge and spin. In this work, the electronic and magnetic structures of $Ga_{1-x}Mn_xAs$ ($x=3.125\%$, 6.25%, 12.5%, 25.0%, 50.0%) are studied by first-principles full-potential linearized augmented plane wave calculations with the generalized-gradient approximation. The ferromagnetic state is lower in energy than the paramagnetic and antiferromagnetic states. It is confirmed that Mn atoms stay magnetic with well localized magnetic moments. The calculated band structure shows that Mn doping also forms defect bands, and makes (Ga,Mn)As *p*-type conducting by providing holes. Furthermore, an *s*-*d* population inversion is found in the Mn electronic configuration, which results from the strong Mn *p*-*d* mixing. The induced As moments are substantial (about $-0.15\mu_B$ per Mn atom, and almost independent of x)—in accord with a recent observed negative As magnetic circular dichroism signal.

DOI: 10.1103/PhysRevB.64.035207 PACS number(s): 75.50.Pp

I. INTRODUCTION

Magnetic semiconductors have attracted considerable attention from experimentists and theorists for several decades,[1] because of the possibility of harnessing the spin of the electron—in addition to its charge—for future semiconductor devices. However, the difficulty of doping to create *p*- and *n*-type diluted magnetic semiconductors (DMS) made the II-VI materials less attractive,[2] until the realization of making III-V semiconductors magnetic, and even ferromagnetic, by introducing a high concentration of magnetic ions. In particular, there is rapidly growing interest in high concentration (Ga,Mn)As, because of its relatively high T_C (110 K) coupled with ferromagnetism.[2–7] $Ga_{1-x}Mn_xAs$ and related semiconductors are under intense investigation for the purpose of understanding the ferromagnetism in these materials, pursuing higher T_C and, finally, for realizing semiconductor electronic devices that use both charge and spin.

The structure of (Ga,Mn)As has been well studied experimentally. At low concentration, the lattice constant of $Ga_{1-x}Mn_xAs$ was found to increase linearly with x, which suggests that all of the Mn atoms are incorporated in Ga sites in the zinc-blende alloy[3]—as confirmed directly by extended x-ray absorption fine-structure measurements.[8] The first-principles calculations done by Shirai *et al.* also support the linear increase of the $Ga_{1-x}Mn_xAs$ lattice constant with x. Mn in $Ga_{1-x}Mn_xAs$ provides both localized spins and holes, due to its magnetic and acceptor nature. It is believed that the appearance of ferromagnetism is caused by the magnetic interaction mediated by the high concentration of holes introduced by Mn.[10]

Several theoretical calculations have been done on (Ga,Mn)As and (In,Mn)As recently. Akai[11] studied the stability of (In,Mn)As with the Korringa-Kohn-Rostoker coherent-potential approximation and local density approximation (LDA). T. Ogawa, *et al.*[12] employed first-principles linear muffin-tin orbital (LMTO) atomic sphere approximation (ASA) band calculations for $Ga_{1-x}Mn_xAs$ ($x=1.0$, 0.25, and 0.125), and they found that the magnetic spin moment is $4\mu_B$ per Mn atom and antiferromagnetic (AFM) coupling between Mn and nearby As moments. Later, Sanvito *et al.*[13] investigated a wide range of Mn concentrations, from $x=1.0$ to 0.02, in $Ga_{1-x}Mn_xAs$ by a linear combination of atomic orbitals (LCAO) method within the LDA. They suggested that the mean field approximation breaks down in Mn-doped GaAs, and a calculation on the corrections due to multiple scattering was attempted. Furthermore, Sanvito and Hill[14] also investigated the effect of the inclusion of As antisites in the diluted (Ga,Mn)As.

In this paper, we employed the highly precise first-principles full-potential linearized augmented plane wave method[15] (FLAPW) within the generalized-gradient approximation (GGA) to investigate further the electronic and magnetic properties of $Ga_{1-x}Mn_xAs$ with low and high Mn concentrations of 50.0%, 25.0%, 12.5%, 6.25%, and 3.125%. The FM state is found to be the stablest state for all x, by a large energy difference from AFM. Moreover, strong Mn *p*-*d* mixing is found, which results in an *s*-*d* population inversion.

II. COMPUTATIONAL DETAILS

In the FLAPW method, there is no artificial shape approximation for the wave functions, charge density, and potential. For all the Ga, Mn, As atoms, the core states are treated fully relativistically and the valence states are treated semirelativistically (i.e., without spin-orbit coupling). The GGA formulas for the exchange-correlation potential are from Perdew *et al.*[16] Muffin-tin (MT) radii for both Mn and Ga were chosen as 2.63 a.u., while it was 2.00 a.u. for As. An energy cutoff of 7.3 Ry was employed for the augmented plane-wave basis to describe the wave functions in the interstitial region, and a 49 Ry cutoff was used for the star functions depicting the charge density and potential. Within the MT spheres, lattice harmonics with angular momentum l up to 8 were adopted.

Sizes of unit cells, as well as corresponding lattice constants, are listed in Table I for each Mn concentration. For

TABLE I. Lattice constants extrapolated from experimental results and the size of unit cells used in PM and FM calculations for different concentrations of Mn. In the AFM calculation, the volume of the unit cell is doubled except for $x=50.0\%$. The AFM configurations of Mn in spin superlattices are decribed in period p and layer orientation **G**.

x(%)	3.125	6.250	12.50	25.00	50.00
a (Å)	5.666	5.676	5.696	5.736	5.816
$x\times y\times z$ (a)	$2\times2\times2$	$1\times2\times2$	$1\times1\times2$	$1\times1\times1$	$1\times1\times1$
k mesh	$2\times2\times2$	$4\times2\times2$	$4\times4\times2$	$4\times4\times4$	$4\times4\times4$
p, **G**		1, [100]	1, [100]	1, [001]	1, [100]

low concentrations, the lattice constants of $Ga_{1-x}Mn_xAs$, obtained from interpolation and extrapolation of the experimental values,[3] increase linearly with Mn concentration, x. It has been confirmed that Mn is substitutionally incorporated into the Ga sublattice,[2] so the atoms in the unit cell are arranged in the zinc-blende structure as GaAs except that the impurity Mn atoms substitute Ga atoms. As many as 64 atoms are contained in the unit cell for $x=3.125\%$, which together with that for $x=25.0\%$ have the highest symmetry, as they have equivalent axes along $\hat{x}$, $\hat{y}$, and $\hat{z}$. The reciprocal space mesh of $4\times4\times4$ is used for the $1\times1\times1$ unit cells. It includes 64 effective k points in the Brillouin zone, and the total energy of ferromagnetic (FM) $Ga_{1-x}Mn_xAs$, for instance, at $x=0.25$, changes only less than 1.0 meV when the number of effective k points is increased to 216 (with a $6\times6\times6$ mesh). This indicates that the total energy is well predicted with the $4\times4\times4$ k mesh for a $1\times1\times1$ unit cell. Equivalent reciprocal space meshes, i.e, with the inverse ratio to the real space sizes, are employed for different real space unit cells, as listed in Table I. Furthermore, the detailed Mn configurations for antiferromagnetic coupling calculated in this work are decribed as spin superlattices of period p and layer orientation **G** in Table I.

The internal degrees of freedom are not optimized during the calculations. The calculated maximum force is less than 0.014 Ry/bohr and is exerted on As atoms nearest to the Mn atom. Such a force is expected to result in an atomic displacement of about 0.03 a.u., which indicates that the internal structure optimization is not important for the $Ga_{1-x}Mn_xAs$ system.

III. RESULTS AND DISCUSSION

The calculated total energies of the system with paramagnetic (PM), ferromagnetic (FM), and antiferromagnetic (AFM) treatments and the energy differences between them are presented in Table II. For all compositions, the PM state is 1.24 eV or more higher than the FM state, and the AFM state is also 0.12 eV or more higher than the FM state. The fact that the FM state has the lowest energy theoretically agrees with the well-known experimental magnetic state of $Ga_{1-x}Mn_xAs$. Generally, the energy difference between PM and FM increases with Mn concentration. The energy difference between AFM and FM also increases from $x=6.25\%$ to 50.0%. The large energy difference between FM and AFM, which increases with composition for $x\leqslant50\%$, shows that $Ga_{1-x}Mn_xAs$ is very stable with ferromagnetic coupling, and so may be a good candidate for promoting T_C to high temperature. Unfortunately, Mn is thought to form MnAs clusters with NiAs-type structure for $x>7\%$.[17]

TABLE II. Comparison of the total energy (in eV) for the PM, FM, and AFM states of $Ga_{1-x}Mn_xAs$ per Mn atom at different compositions. The energy of the FM state is set to zero.

x(%)	3.125	6.250	12.50	25.00	50.00
PM	1.25	1.24	1.34	1.49	1.51
AFM		0.12	0.14	0.17	0.24

The calculated Mn, Ga, and As magnetic moments in their corresponding muffin-tin spheres in the FM state are shown in Table III. Ga and As atoms are listed in the order of their distance from the Mn atom. There are two types of Ga1 atoms, marked as Ga1-1 and Ga1-2, located at $\sqrt{2}a/2$ with respect to the Mn atom for a concentration of 6.25% and 12.5%. Ga1-1 is at the boundary of the unit cell along the shorter axis, $\hat{x}$, in the case of 6.25%, and along $\hat{x}$, $\hat{y}$ in the

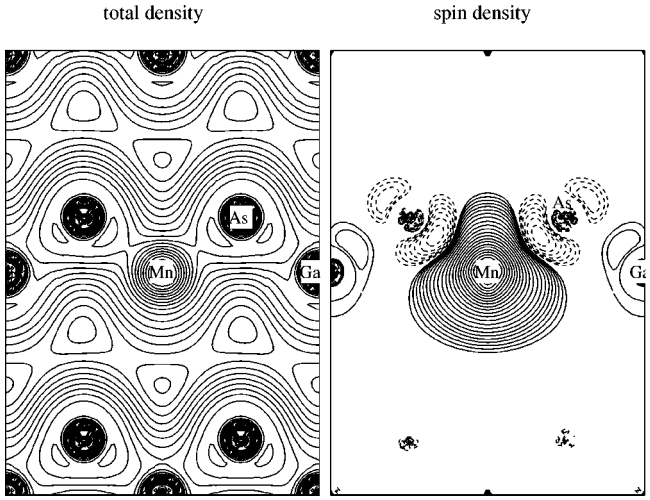

FIG. 1. Valence charge density (left) and spin density of $Ga_{1-x}Mn_xAs$ at $x=6.25\%$, plotted in the (110) plane with Mn at the center. The contours of total valence charge density are plotted as $\rho=0.01\times2^{(n-1)/2}e/\text{bohr}^3$. Spin density contours are plotted as $\rho=0.0005\times2^{(n-1)/2}e/\text{bohr}^3$. Here, n represents the nth contour line from the lowest density zone. For the spin density, spin up is represented by solid lines, while spin down is represented by dashed lines.

TABLE III. The calculated magnetic moment (μ_B) in the muffin-tin spheres. Ga and As atoms are listed in the order of their distance from Mn (d-Mn, with unit of lattice constant a) with total moments over the number of atoms of the type. If there are different types with the same distance from Mn, the ones with more neighbor Mn atoms are listed first. The total spin moment of interstitial region is also listed, which is denoted as ''inter.''

x(%)	Mn	Ga1	Ga2	Ga3	Ga4	Ga5	As1	As2	As3	As4	inter
d-Mn	–	$\sqrt{2}/2$	1	$\sqrt{6}/2$	$\sqrt{2}$	$\sqrt{3}$	$\sqrt{3}/4$	$\sqrt{11}/4$	$\sqrt{19}/4$	$3\sqrt{3}/4$	–
3.125	3.80	0.12/12	0.00/3	-0.01/12	0.00/3	0.00/1	-0.10/4	-0.03/12	-0.02/12	-0.02/4	0.24
6.250	3.77	0.08/4 0.03/4	0.01/2	-0.01/4	0.00/1	–	-0.10/4	-0.03/8	-0.03/4	–	0.27
12.50	3.79	0.03/1 0.08/4	0.01/1	0.00/1	–	–	-0.13/4	-0.01/4	–	–	0.23
25.00	3.82	0.11/3	–	–	–	–	-0.15/4	–	–	–	0.21
50.00	3.90	0.07/1	–	–	–	–	-0.14/2	–	–	–	0.33

case of 12.5%. Ga1-1 has two neighboring Mn atoms at a distance of $\sqrt{2}a/2$, while Ga1-2 has only one. The spin density at $x=6.25\%$ is shown in Fig. 1; it is very similar for all concentrations. From Table III, it is known that spin moments are strongly localized in the Mn MT spheres. This can be seen more clearly from the spin density distribution (cf. Fig. 1), which indicates that the spin density is less than 10^{-2} μ_B/bohr^3 outside of the Mn sphere with a radius of 0.63 Å. The calculated magnetic moment in the Mn MT sphere increases nearly linearly with x from 6.25% to 50.0%. The Mn spin moments obtained by Ogawa *et al.*[12] are $3.79\mu_B$ and $3.84\mu_B$ for $x=12.5\%$ and 25.0% respectively, where they used the same lattice constants and a very close Mn atomic sphere radius ($\sim$2.60 a.u. versus 2.63 a.u.) compared with our work. Their results are in very good agreement with our values of $3.79\mu_B$ and $3.82\mu_B$, respectively. This indicates that LDA and GGA agree with each other very well in the description of magnetic properties for a given $Ga_{1-x}Mn_xAs$ structure. The slight Mn moment decrease from 3.125% to 6.25% may be due to the abrupt decrease of the nearest Mn distance, $2a \rightarrow a$, in the calculation, and is also why the PM-FM energy splitting and other properties show ''anomalies'' at $x=3.125\%$. The total valence charge density (cf. Fig. 1) shows that the Mn-As bonds are stronger than those of Ga-As.

The magnetic moment is essentially of Mn $3d$ origin; Mn $4s$ and $4p$ polarizations are very weak, which can be seen from Mn $3d$, $4s$, and $4p$ electron populations in Table IV.

TABLE IV. Electron populations of Mn in the muffin-tin sphere (i.e, the overlap populations are neglected) at different Mn compositions.

x(%)	3.125	6.250	12.50	25.00	50.00
$3d\uparrow$	4.465	4.449	4.463	4.469	4.490
$3d\downarrow$	0.790	0.807	0.783	0.757	0.700
$4s\uparrow$	0.266	0.266	0.267	0.268	0.267
$4s\downarrow$	0.219	0.217	0.217	0.214	0.202
$4p\uparrow$	0.296	0.297	0.280	0.269	0.242
$4p\downarrow$	0.216	0.211	0.212	0.205	0.191
Total	6.252	6.247	6.222	6.182	6.092

The Mn $4s$ polarization is 0.047 at $x=3.125\%$, and increases steadily to 0.065 as x increases to 50.0%; in contrast, the Mn $4p$ polarization decreases from 0.080 to 0.043. Mn may be considered as neutral if the shared electrons in the interstitial region are taken into account. The electron population in the Mn MT sphere of Mn decrease linearly from 6.252 to 6.092 with x. Surprisingly, the total d electronic population within the MT sphere is around 5.2, more than that in the free Mn atom. This could be called s-d population

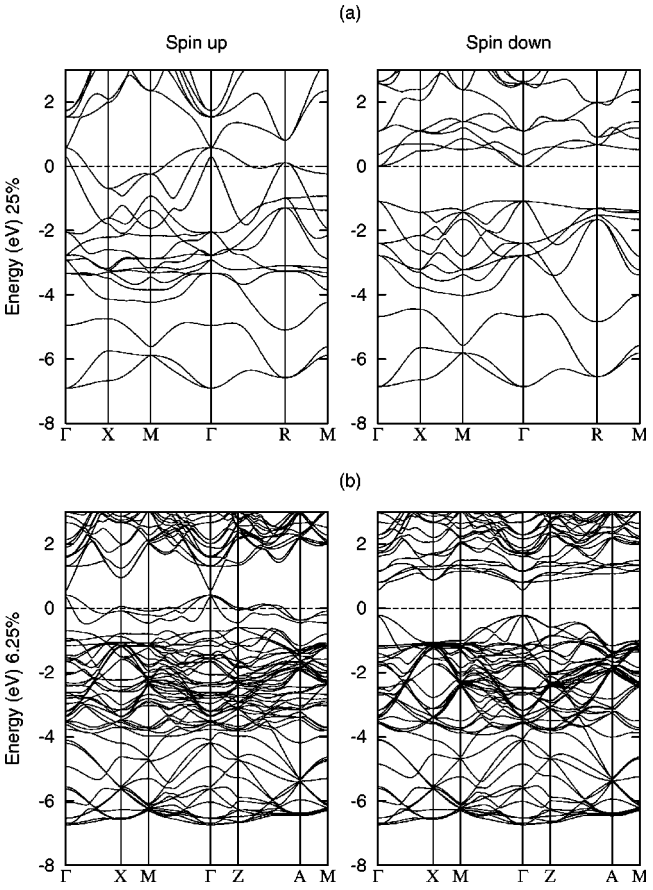

FIG. 2. Band structures of $Ga_{1-x}Mn_xAs$ at (a) $x=25.0\%$ and (b) 6.25%. The horizontal line denotes the position of the Fermi energy, which has been chosen to be 0 eV.

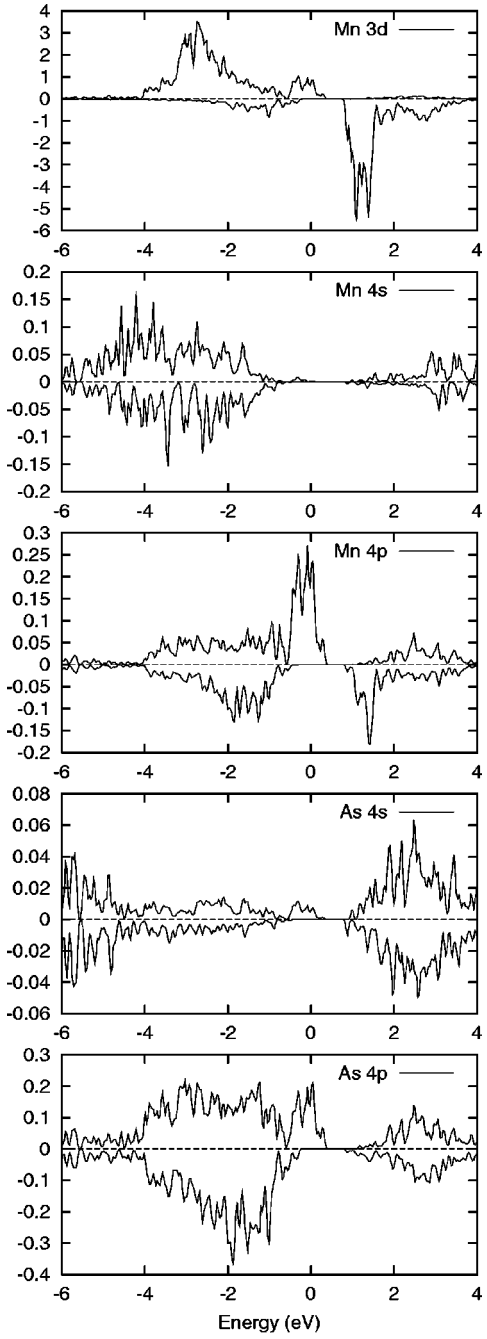

FIG. 3. Mn $3d$, $4s$, $4p$, and the nearest As $4s$ $4p$ density of states for $x=6.25\%$, which is plotted using a Gaussian broadening technique with a parameter of 0.04 eV. The Fermi level is set as zero and the unit of DOS is $(\text{eV atom})^{-1}$.

inversion, i.e., an $s\rightarrow d$ promotion. This picture is in marked contradiction to the Woodbury-Ludwig model,[18] which hypothesized for substitutional $3d$ elements in zinc-blende alloys, that the $3d$ electrons would be promoted into the sp subshell to form a tetrahedral hybrid (i.e., $d^n s^2 \rightarrow d^{n-2} s^1 p^3$, or $d^n s^1 \rightarrow d^{n-3} s^1 p^3$). Then how do Mn atoms complete the tetrahedral bonds with nearest As atoms? That is not a simple sp hybridization for transition-atom impurities, as Zunger pointed out.[19] The discrete atomic energy levels of the impurity atom undergo substantial changes in the solid.

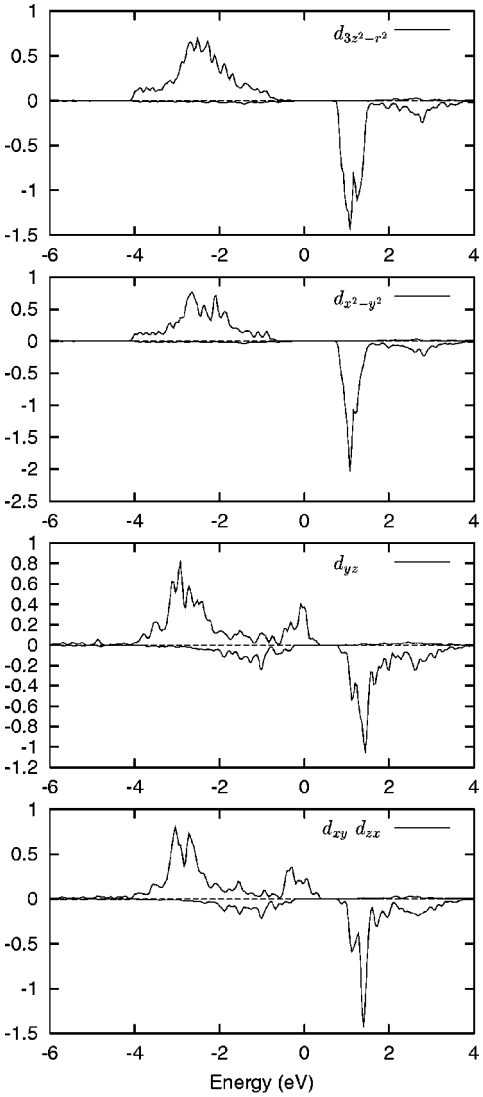

FIG. 4. Projection of Mn $3d$ density of states for e and t_2 levels for $x=6.25\%$, which is plotted using Gaussian broadening technique with a parameter of 0.04 eV. The Fermi level is set as zero and the unit of DOS is $(\text{eV atom})^{-1}$.

The impurity's final effective charge density corresponds to that of a compressed atom with its s electrons excited into the p and d shells. Our result also supports the suggestion of an $s\rightarrow d$ promotion for $3d$ interstitial impurities in semiconductors, which gives a simple explanation for the diffusion puzzle in the Si:Ni and Si:Ti systems.[20] In Ref. 13, the total population for the d orbital of Mn is around 5.5 electronic charges, which is larger than our results since their value includes the overlap populations. The s-d population inversion in $Ga_{1-x}Mn_xAs$ is also found in our LCAO DMOL[3] calculations.[21] Actually, in the case of substitutional transition-atom impurities in Si, an $s\rightarrow d$ crossover has been reported,[19] which also contradicts the Ludwig-Woodbury model.

The nearby Ga atoms contribute a small positive spin moment, while the As atoms give a negative contribution—amounting to nearly $-0.15\mu_B$ per Mn atom, which is almost independent of x. This is in accord with the fact that a nega-

tive MCD signal was observed in a recent experiment of Beschoten *et al.*[22] The negative As spin density is located in front and back of the atom along the Mn-As line (cf. Fig. 1), which shows its p character; the As $4s$ contribution is negligible. The Ga $4s$ and $4p$ contribute almost equally to the spin moment, and makes the spin density curves near Ga quite different from those near As. The spin moments of Ga and As induced by Mn atoms diminish as the concentration of Mn decreases, or with their distance to the Mn atom. Considering the contributions from the interstitial region, the total spin moment of the unit cell is exactly $4.0\mu_B$—which results from the half-metallic ferromagnetic nature of the energy gap in the spin-down band structure shown in next paragraph. This is in accord with previous theoretical calculations.[9,12,13] While it is not easy to determine spin moments from the experiments, $4.4\mu_B$ was estimated for Mn in $Ga_{1-x}Mn_xAs$ with $x=3.5\%$ at a temperature of 5 K by Ohno *et al.*[3]

The $Ga_{1-x}Mn_xAs$ band structures for $x=6.25\%$ and 25.0% are shown in Fig. 2. The bottom of the conduction bands and the top of the valence bands are at the Γ point in the Brillouin zone, which is the same as in pure GaAs. In the spin-down panel, E_F is located in the energy gap. It is obvious that both compositions are half-metallic, as is also the case for $x=3.125\%$ and 12.5% (both not shown), but the 25.0% composition is just barely so. The defect bands, which are introduced by the Mn impurities, are clearly seen around E_F in the band plots for $x=6.25\%$. Since holes come from the defect bands, Mn doping of GaAs at Ga sites results in p-type conductivity, along with the introduction of large and well localized magnetic moments. Our first-principles results are in line with experiment for $x=3.125\%$, but not for $x=6.25\%$. Experimentally, $Ga_{1-x}Mn_xAs$ is an insulator at $x=5.3\%$ and 7.1%.[23] This discrepancy might be ascribed to the well-known LDA problem for energy gaps or to a ''random'' distribution of Mn in the experiment. There are no experimental data available for samples with Mn concentration greater than 7.1% where Mn clustering is thought to occur.[17]

The projected density of states (DOS) of Mn $3d$, $4s$, and $4p$ for $x=6.25\%$ in Fig. 3 shows that the spin-up Mn $3d$ levels are almost occupied while most of the spin-down levels lie above E_F. The DOS peaks around E_F from Mn $3d$ and $4p$ indicate their large contributions to the defect bands. Mn $4s$ contributes little to the defect bands because it obviously lies lower in energy than the Mn $3d$ and $4p$. The similar DOS distribution in energy of the Mn $3d$, $4p$ levels shows that they are heavily mixed. To gain a deeper insight into the electronic structure of Mn, we project the $3d$ Mn DOS further into e ($d_{3z^2-r^2}$ and $d_{x^2-y^2}$) and t_2 (d_{xy}, d_{yz}, and d_{zx}) levels in Fig. 4. Obviously, the e levels are highly localized in energy, while the t_2 levels are relatively less so; the relatively large width of the t_2 levels comes from the defect states and the strong mixing with the Mn $4p$ levels allowed by symmetry. It is clear that the $t_2\uparrow$ DOS at E_F is quite high, which indicates that the defect bands comes from Mn $t_2\uparrow$ levels rather than other $3d$ levels. The As $4p$ states also contributes to the defect bands because of the strong interaction with Mn $4p$ levels. Clearly, the exchange splitting energy is much larger than the crystal field splitting energy in this system, which keeps $Ga_{1-x}Mn_xAs$ in the *high spin* level ordering.[24]

IV. SUMMARY

A wide range of Mn concentrations for $Ga_{1-x}Mn_xAs$ systems was studied by the FLAPW method. The FM state is the ground state for $Ga_{1-x}Mn_xAs$ at all Mn compositions; it is $\geqslant 0.12$ eV lower in energy than the AFM, and $\geqslant 1.24$ eV lower than the PM state, which shows that ferromagnetic $Ga_{1-x}Mn_xAs$ is very stable. The total spin moments, whose origin is Mn $3d$ in these $Ga_{1-x}Mn_xAs$ systems, are $4.00\mu_B$. The Mn atom induces small spin moments on the nearby Ga (positive) and substantial ones on the As (negative) atoms, which is in accord with the recently observed negative As MCD signal. It is clear that $Ga_{1-x}Mn_xAs$ has p-type conductivity since holes come from the defect bands. Furthermore, an s-d population inversion is found for Mn, which is caused by the strong Mn p-d mixing.

ACKNOWLEDGMENTS

Work supported by the NSF (through the Materials Research Center at Northwestern University and a computer time grant at the San Diego Supercomputing Center). We thank K. Nakamura for valuable discussions.

*Present address: Kookmin University, Department of Physics, 86-1 Chongnungdong, Songbukgu, Seoul 136-702, Korea.

[1] R.A. Chapman and W.G. Hutchinson, Phys. Rev. Lett. **18**, 443 (1967).
[2] H. Ohno, Science **281**, 951 (1998).
[3] H. Ohno, A. Shen, F. Matsukura, A. Oiwa, A. Endo, S. Katsumoto, and Y. Iye, Appl. Phys. Lett. **69**, 363 (1996).
[4] Y. Ohno, D.K. Young, B. Beschoten, F. Matsukura, H. Ohno, and D.D. Awschalom, Nature (London) **402**, 790 (1999).
[5] T. Dietl, H. Ohno, F. Matsukura, J. Cibert, and D. Ferrand, Science **287**, 1019 (2000).
[6] Y. Ohno, R. Terauchi, F. Matsukura, and H. Ohno, Phys. Rev. Lett. **83**, 4196 (2000).
[7] F. Matsukura, H. Ohno, A. Shen, and Y. Sugawara, Phys. Rev. B **57**, R2037 (1998).
[8] R. Shioda, K. Ando, T. Hayashi, and M. Tanaka, Phys. Rev. B **58**, 1100 (1998).
[9] M. Shirai, T. Ogawa, I. Kitagawa, and N. Suzuki, J. Magn. Magn. Mater. **177-181**, 1383 (1998).
[10] H. Ohno, Physica E (Amsterdam) **6**, 702 (2000).
[11] H. Akai, Phys. Rev. Lett. **81**, 3002 (1998).
[12] T. Ogawa, T. Shirai, N. Suzuki, and I. Kitagawa, J. Magn. Magn. Mater. **196-197**, 428 (1999).
[13] S. Sanvito, P. Ordejón, and N.A. Hill, Phys. Rev. B **63**, 165206 (2001).
[14] S. Sanvito and N.A. Hill, cond-mat/0011372 (unpublished).
[15] E. Wimmer, H. Krakauer, M. Weinert, and A.J. Freeman, Phys. Rev. B **24**, 864 (1981), and references therein.

[16] J.P. Perdew, K. Burke, and M. Ernzerhof, Phys. Rev. Lett. **77**, 3865 (1996).
[17] H. Ohno, J. Magn. Magn. Mater. **200**, 110 (1999).
[18] H.H. Woodbury and G.W. Ludwig, Phys. Rev. **117**, 102 (1960).
[19] Alex Zunger and U. Lindefelt, Phys. Rev. B **27**, 1191 (1983).
[20] E.R. Weber, Appl. Phys. A: Solids Surf. **30**, 1 (1983).
[21] We calculated the $Ga_{1-x}Mn_xAs$ system at $x=25.0\%$ and 12.5% with a first-principles LCAO band structure method, DMOL [3] [cf. B. Delley, J. Chem. Phys. **92**, 508 (1990); **113**, 7756 (2000). It also gives a similar population inversion within a Mulliken population analysis.
[22] B. Beschoten, P.A. Crowell, I. Malajovich, and D.D. Awschalom, Phys. Rev. Lett. **83**, 3073 (1999).
[23] A. Oiwa, S. Katsumoto, A. Endo, M. Hirasawa, Y. Iye, H. Ohno, F. Matsukura, A. Shen, and Y. Sugawara, Solid State Commun. **103**, 209 (1997).
[24] Alex Zunger, Solid State Phys. **39**, 275 (1986).